ASTRONOMY & ASTROPHYSICS
SUPPLEMENT SERIES

Astron. Astrophys. Suppl. Ser. **139**, 617–623 (1999)

The stark broadening effect in hot star atmospheres: Au I and Au II lines

L.Č. Popović, M.S. Dimitrijević, and D. Tankosić

Astronomical Observatory, Volgina 7, 11000 Belgrade, Yugoslavia

Received January 27; accepted June 16, 1999

Abstract. The Stark broadening parameters for six Au I lines and eight Au II transitions have been calculated. Two methods for calculation have been used: the semiclassical method (for Au I lines) and the modified semiempirical approach (for Au II transitions). In the case of Au II, the jj coupling approximation has been used for the matrix-element calculations. The importance of the electron-impact effect in the case of Au II $\lambda = 174.0476$ nm line for several stellar atmosphere models has been tested.

Key words: atomic processes — line formation — stars: atmospheres — stars: early-type

1. Introduction

Hg-Mn stars are nonmagnetic late B type stars that display unusually strong lines of many heavy ions (see e.g. Preston 1971; Heacox 1979; Dworetsky 1980; Dworetsky et al. 1984; Adelman 1987; Wahlgren et al. 1995). E.g. the mercury abundances in this type of stars are between 4000 and 40000 times larger than solar ones (see e.g. Aller & Ross 1967; Sargent 1964). In A and B type stars the electron-impact broadening is the main pressure broadening mechanism (e.g. Dimitrijević 1989). Considering that the resonant lines of ionized heavy elements ($z > 30$) are located in the ultraviolet spectral region, the abundance analysis of these elements has become possible due to satellite observations by high resolution spectrographs as e.g. International Ultraviolet Explorer (IUE) satellite ($R = 12000$) or Goddard High Resolution Spectrograph (GHSR) installed at Hubble Space Telescope. The number of heavy ion lines observations with the higher photometric quality and spectral resolution is growing up. Consequently, experimental and theoretical spectroscopic data for modelling of these lines are required.

In order to investigate the Hg-Mn star atmospheres as well as other types of hot stars, the Stark broadening parameters for heavy ion lines are needed. The most sophisticated theoretical method for the calculation of a Stark broadened line profile is of course the quantum mechanical close coupling approach. However, due to its complexity and numerical difficulties, only a small number of such calculations exist. In a lot of cases, such as e.g. the transitions between more excited energy levels, the more sophisticated quantum mechanical approach is very difficult or even practically impossible to use and the semiclassical approach (e.g. Sahal-Bréchot 1969a,b) remains the most efficient method for Stark broadening calculations. But for radiators with complex spectra, heavy elements or multiply charged ions, even the semiclassical method is often not applicable in an adequate way due to the lack of reliable data on atomic energy levels, or due to the complexity of the spectrum, problems of level mixing or problems with the adequate identification of atomic energy levels. Simpler approaches are as well of interest when line broadening data for a large number of lines are required (e.g. opacity calculations), and the high precision of every particular result is not so important, but only a good average accuracy is sufficient.

Here we present the electron-impact broadening parameters for six Au I lines and eight Au II transitions as a function of temperature, calculated by using the semiclassical (Sahal-Bréchot 1969a,b) and modified semiempirical approach (Dimitrijević & Konjević 1980; Dimitrijević & Kršljanin 1986; Popović & Dimitrijević 1996), respectively.

The Au II lines are observed in Hg-Mn and other CP stars (Wahlgren et al. 1995; Fuhrmann 1988; Adelman 1994). The investigation of gold in Hg-Mn stars shows that the abundances, obtained from the Au II λ174.0476 nm line, are between 4000 (for χ Lup) and 20000 (for k Cnc) times larger than solar ones (Wahlgren et al. 1995).

Send offprint requests to: L.Č. Popović,
e-mail: lpopovic@aob.bg.ac.yu

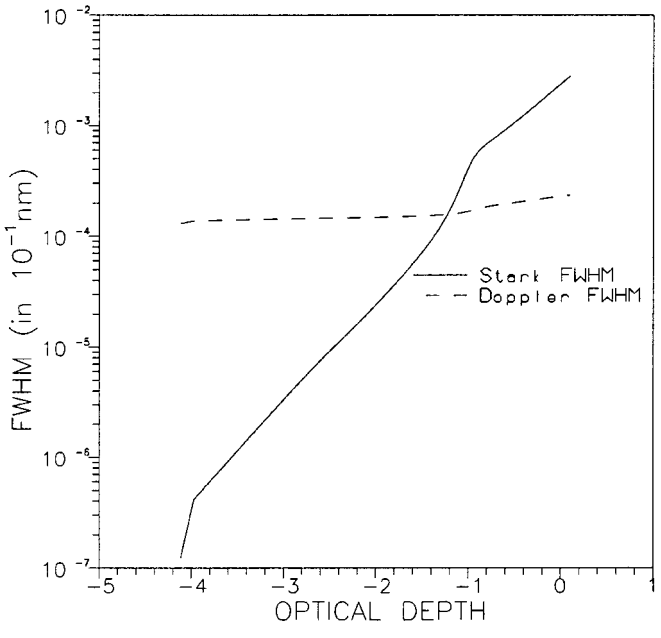

Fig. 1. Thermal Doppler and Stark widths for Au II (λ = 174.048 nm) line as functions of optical depth for an A type star ($T_{\rm eff}$ = 10000 K, $\log g = 4$)

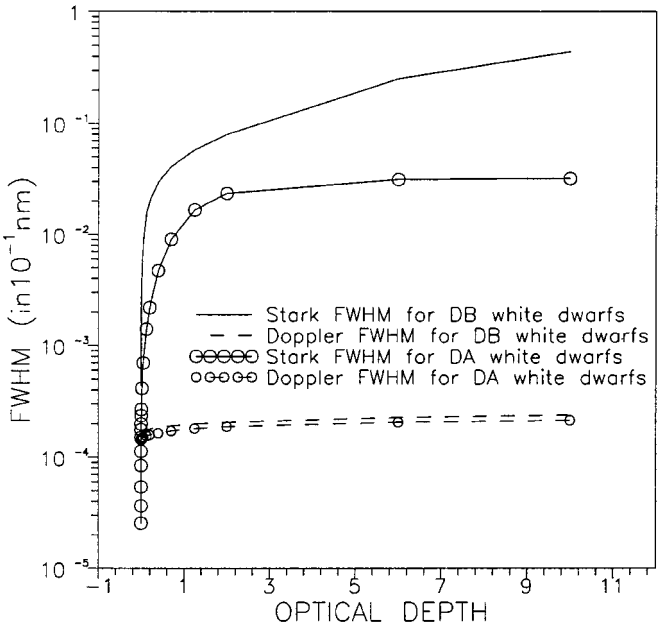

Fig. 2. Same as in Fig. 1, but for DA ($T_{\rm eff}$ = 10000 K, $\log g = 6$, curves with circles) and DB ($T_{\rm eff}$ = 15000 K, $\log g = 7$) white dwarfs

Since a sufficiently complete set of reliable atomic data needed for the application of the full semiclassical - perturbation approach (Sahal-Bréchot 1969a,b) in an adequate way does not exist, the modified semiempirical method (Dimitrijević & Konjević 1980; Dimitrijević & Kršljanin 1986; Popović & Dimitrijević 1996) has been used for Stark broadening calculation of Au II lines, whereas for Au I lines the more sophisticated semiclasical perturbation approach (Sahal-Bréchot 1969a,b) has been applied.

2. Results and discussion

For Au I spectral lines Stark broadening parameters, the full semiclassical perturbation formalism (Sahal-Bréchot 1969a,b), has been applied. A summary of the formalism for neutral emitters is given in Dimitrijević & Sahal-Bréchot (1984), and for ionized in Dimitrijević et al. (1991) and Dimitrijević & Sahal-Bréchot (1996). We note here that the inelastic collision contribution is included in the ion-impact line widths.

Energy levels for Au I lines have been taken from Moore (1971). Oscillator strengths have been calculated by using the method of Bates & Damgaard (1949) and the tables of Oertel & Shomo (1968). For higher levels, the method described by Van Regemorter et al. (1979) has been used. In addition to electron-impact full halfwidths and shifts, Stark-broadening parameters due to proton-, and He II- impacts have been calculated. Our results for six Au I lines are shown in Table 1, for perturber densities $10^{15} - 10^{19}$ cm^{-3} and temperatures $T = 2\,500 - 50\,000$ K. We also specify a parameter C (Dimitrijević & Sahal-Bréchot 1984), which gives an estimate for the maximum perturber density for which the line may be treated as isolated when it is divided by the corresponding full width at half maximum. For each value given in Table 1, the collision volume (V) multiplied by the perturber density (N) is much less than one and the impact approximation is valid (Sahal-Bréchot 1969a,b). Values for $NV > 0.5$ are not given and values for $0.1 < NV \leq 0.5$ are denoted by an asterisk. Tabulated Stark broadening parameters are linear with perturber density for perturber densities lower than 10^{15} cm^{-3}. The accuracy of the semiclasical method is $\pm$ 30% (Griem 1974). When the impact approximation is not valid, the ion broadening contribution may be estimated by using quasistatic approach (Sahal-Bréchot 1991 and Griem 1974). In the region between, where neither of these two approximations is valid, a unified type theory should be used. For example in Barnard et al. (1974), a simple analytical formulas for such a case are given. The accuracy of the results obtained decreases when broadening by ion interactions becomes important.

For Au II spectral lines, the electron-impact broadening calculation has been performed within the modified semiempirical approach. Considering the very complex spectrum of Au II, the jj coupling approximation for matrix-element calculation has been used. The needed atomic data for calculation have been taken from Rosberg & Wyart (1996). In Table 2, the electron-impact parameteres for eight Au II transitions as a function of temperature for an electron density of $N_{\rm e} = 10^{17}$ cm^3 are presented. The average accuracy of the MSE method is $\pm$ 50% (Dimitrijević & Konjević 1980).

In order to see the influence of Stark broadening mechanism for gold spectral lines in stellar plasma, we have

calculated the Stark widths for Au II $\lambda = 174.0476$ nm throught the different models of stellar atmospheres. In Figs. 1 and 2, the electron-impact and thermal Doppler widths as function of optical depth for Kurucz's (1979) A type star ($T_{\rm eff} = 10000$ K, $\log g = 4$) and models of DA ($T_{\rm eff} = 10000$ K, $\log g = 6$) and DB ($T_{\rm eff} = 15000$ K, $\log g = 7$) white dwarf atmospheres (Wickramasinghe 1972) are presented. As one can see from Fig. 1, for the case of hot A type star, in photospheric layers the line width due to Stark broadening is one order of magnitude larger than the width due to the thermal Doppler mechanism. In higher layers of the stellar atmosphere ($\tau \approx -4$) however, the thermal Doppler mechanism is more important. In the case of white dwarf atmospheres (see Fig. 2) the Stark broadening mechanism is important in all layers of atmospheres and in deeper atmosphere layers the Stark width is two or three order of magnitude larger than thermal Doppler width. For the three here considered atmosphere models Stark broadening effect should be taken into account in abundance determination and other investigations of stellar plasmas.

Acknowledgements. This work is a part of the project "Astrometrical, Astrodynamical and Astrophysical Investigations", supported by Ministry of Science and Technology of Serbia.

References

Adelman S.J., 1987, MNRAS 228, 573
Adelman S.J., 1994, MNRAS 266, 97
Aller L.H., Ross J.E., 1967, The Magnetic and Related Stars, Cameron R.C. (ed.). Baltimor, p. 339
Barnard A.J., Cooper J., Smith E.W., 1974, JQSRT 14, 1025
Bates D.R., Damgaard A., 1949, Trans. Roy. Soc. London, Ser. A 242, 101
Dimitrijević M.S., 1989, Bull. Obs. Astron. Belgrade 140, 111
Dimitrijević M.S., Konjević N., 1980, JQSRT 24, 454
Dimitrijević M.S., Kršljanin V., 1986, A&A 165, 269
Dimitrijević M.S., Sahal-Bréchot S., 1984, JQSRT 31, 301
Dimitrijević M.S., Sahal-Bréchot S., 1996, Phys. Scr. 54, 50
Dimitrijević M.S., Sahal-Bréchot S., Bommier V., 1991, A&AS 89, 581
Dworetsky M.M., 1980, A&A 84, 350
Dworetsky M.M., Storey P.J., Jacobs J.M., 1984, Phys. Scr. 8, 39
Griem H.R., 1974, Spectral Line Broadening by Plasmas. Academic Press, New York
Heacox W.D., 1979, ApJSS 41, 675
Fuhrmann K., 1988, ESA Spec. Publ 281, 1, 405
Kurucz R.L., 1979, ApJSS 40, 1
Moore C.E., 1971, Atomic Energy Levels Vol. III, NSRDS-NBS 35, Washington
Oertel G.K., Shomo L.P., 1968, ApJSS 16, 175
Preston G.W., 1971, PASP 83, 571
Popović L.Č., Dimitrijević M.S., 1996, Phys. Scr. 53, 325
Rosberg M., Wyart J.-F., 1996, Phys. Scr. 55, 690
Sahal-Bréchot S., 1969a, A&A 1, 91
Sahal-Bréchot S., 1969b, A&A 2, 322
Sahal-Bréchot S., 1991, A&A 245, 322
Sargent W.L., 1964, ARA&A 2, 297
Van Regemorter H., Hoang Binh Dy, Prud'homme M., 1979, J. Phys. B 12, 1073
Wahlgren G.M., Leckrone D.S., Johansson S.G., Rosberg M., Brage T., 1995, ApJ 444, 438
Wickramasinghe D.T., 1972, Mem. R. Astron. Soc. 76, 129

Table 1. This table shows electron-, proton-, and He II- impact broadening parameters for Au I, calculated within the full semiclassical perturbation approach (Sahal-Bréchot 1969a,b) for perturber densities of $10^{15} - 10^{19}$ cm^{-3} and temperatures from 2 500 up to 50 000 K. Transitions and averaged wavelengths for the multiplet (in nm) are also given. By dividing C by the corresponding full width at half maximum (Dimitrijević et al. 1991), we obtain an estimate for the maximum perturber density for which the line may be treated as isolated and tabulated data may be used. The asterisk identifies cases for which the collision volume multiplied by the perturber density (the condition for validity of the impact approximation) lies between 0.1 and 0.5. Stark broadening parameters for densities lower than tabulated, are linear with perturber density

PERTURBER DENSITY= 1.E+15cm-3							
PERTURBERS ARE:		ELECTRONS		PROTONS		IONIZED HELIUM	
TRANSITION	T(K)	W (0.1nm)	d (0.1nm)	W (0.1nm)	d (0.1nm)	W (0.1nm)	d (0.1nm)
6s2S-6p2Po1/2	2500.	0.144E-03	0.602E-04	0.957E-04	0.166E-04	0.955E-04	0.132E-04
Au I 267.67 nm	5000.	0.167E-03	0.690E-04	0.959E-04	0.186E-04	0.956E-04	0.148E-04
C=0.12E+19	10000.	0.175E-03	0.701E-04	0.961E-04	0.210E-04	0.957E-04	0.167E-04
	20000.	0.191E-03	0.627E-04	0.964E-04	0.236E-04	0.959E-04	0.188E-04
	30000.	0.213E-03	0.496E-04	0.966E-04	0.252E-04	0.960E-04	0.201E-04
	50000.	0.259E-03	0.360E-04	0.970E-04	0.275E-04	0.962E-04	0.219E-04
6s2S-6p2Po3/2	2500.	0.164E-03	0.101E-03	0.104E-03	0.278E-04	0.103E-03	0.221E-04
Au I 242.87 nm	5000.	0.192E-03	0.120E-03	0.105E-03	0.313E-04	0.104E-03	0.249E-04
C=0.79E+18	10000.	0.209E-03	0.132E-03	0.106E-03	0.352E-04	0.104E-03	0.280E-04
	20000.	0.230E-03	0.133E-03	0.107E-03	0.396E-04	0.105E-03	0.315E-04
	30000.	0.254E-03	0.134E-03	0.108E-03	0.424E-04	0.105E-03	0.338E-04
	50000.	0.295E-03	0.109E-03	0.109E-03	0.462E-04	0.106E-03	0.368E-04
6s2S-7p2Po1/2	2500.	0.117E-02	0.844E-03	0.381E-03	0.217E-03	0.356E-03	0.171E-03
Au I 166.58 nm	5000.	0.131E-02	0.965E-03	0.400E-03	0.248E-03	0.368E-03	0.196E-03
C=0.53E+17	10000.	0.145E-02	0.100E-02	0.422E-03	0.282E-03	0.382E-03	0.223E-03
	20000.	0.160E-02	0.917E-03	0.448E-03	0.319E-03	0.400E-03	0.253E-03
	30000.	0.171E-02	0.805E-03	0.466E-03	0.342E-03	0.413E-03	0.272E-03
	50000.	0.184E-02	0.672E-03	0.491E-03	0.373E-03	0.430E-03	0.297E-03
6s2S-7p2Po3/2	2500.	0.154E-02	0.114E-02	0.454E-03	0.290E-03	0.412E-03	0.228E-03
Au I 164.67 nm	5000.	0.172E-02	0.127E-02	0.483E-03	0.333E-03	0.432E-03	0.263E-03
C=0.33E+17	10000.	0.187E-02	0.127E-02	0.517E-03	0.379E-03	0.456E-03	0.300E-03
	20000.	0.202E-02	0.113E-02	0.558E-03	0.430E-03	0.484E-03	0.341E-03
	30000.	0.212E-02	0.990E-03	0.586E-03	0.461E-03	0.503E-03	0.366E-03
	50000.	0.222E-02	0.825E-03	0.626E-03	0.503E-03	0.530E-03	0.400E-03
6s2S-8p2Po1/2	2500.	0.403E-02	0.288E-02	0.119E-02	0.699E-03	*0.108E-02	*0.542E-03
Au I 150.14 nm	5000.	0.453E-02	0.326E-02	0.126E-02	0.817E-03	0.114E-02	0.640E-03
C=0.19E+17	10000.	0.501E-02	0.327E-02	0.134E-02	0.939E-03	0.119E-02	0.740E-03
	20000.	0.558E-02	0.279E-02	0.144E-02	0.107E-02	0.126E-02	0.847E-03
	30000.	0.600E-02	0.242E-02	0.150E-02	0.115E-02	0.131E-02	0.913E-03
	50000.	0.642E-02	0.201E-02	0.160E-02	0.126E-02	0.137E-02	0.100E-02
6s2S-8p2Po1/2	2500.	0.550E-02	0.396E-02	0.146E-02	0.949E-03	*0.129E-02	*0.731E-03
Au I 149.45 nm	5000.	0.605E-02	0.432E-02	0.157E-02	0.112E-02	*0.137E-02	*0.872E-03
C=0.12E+17	10000.	0.651E-02	0.419E-02	0.170E-02	0.129E-02	0.146E-02	0.102E-02
	20000.	0.705E-02	0.346E-02	0.185E-02	0.147E-02	0.157E-02	0.117E-02
	30000.	0.741E-02	0.297E-02	0.196E-02	0.159E-02	0.164E-02	0.126E-02
	50000.	0.770E-02	0.246E-02	0.210E-02	0.174E-02	0.175E-02	0.138E-02
PERTURBER DENSITY= 1.E+16cm-3							
6s2S-6p2Po1/2	2500.	0.144E-02	0.600E-03	0.956E-03	0.163E-03	0.952E-03	0.129E-03
Au I 267.67 nm	5000.	0.167E-02	0.688E-03	0.958E-03	0.185E-03	0.955E-03	0.146E-03
C=0.12E+20	10000.	0.175E-02	0.700E-03	0.961E-03	0.209E-03	0.957E-03	0.166E-03
	20000.	0.191E-02	0.627E-03	0.964E-03	0.235E-03	0.959E-03	0.187E-03
	30000.	0.213E-02	0.496E-03	0.966E-03	0.251E-03	0.960E-03	0.200E-03
	50000.	0.259E-02	0.360E-03	0.970E-03	0.274E-03	0.962E-03	0.218E-03
6s2S-6p2Po3/2	2500.	0.164E-02	0.101E-02	0.104E-02	0.271E-03	0.103E-02	0.214E-03
Au I 242.87 nm	5000.	0.192E-02	0.119E-02	0.105E-02	0.308E-03	0.104E-02	0.244E-03
C=0.79E+19	10000.	0.209E-02	0.132E-02	0.106E-02	0.349E-03	0.104E-02	0.277E-03
	20000.	0.230E-02	0.133E-02	0.107E-02	0.394E-03	0.105E-02	0.313E-03
	30000.	0.254E-02	0.134E-02	0.108E-02	0.422E-03	0.105E-02	0.336E-03
	50000.	0.295E-02	0.109E-02	0.109E-02	0.461E-03	0.106E-02	0.367E-03
6s2S-7p2Po1/2	2500.	0.117E-01	0.820E-02	0.377E-02	0.193E-02	*0.348E-02	*0.147E-02
Au I 166.58 nm	5000.	0.131E-01	0.949E-02	0.398E-02	0.231E-02	*0.365E-02	*0.179E-02
C=0.53E+18	10000.	0.145E-01	0.993E-02	0.421E-02	0.270E-02	0.381E-02	0.212E-02
	20000.	0.160E-01	0.916E-02	0.448E-02	0.310E-02	0.400E-02	0.245E-02
	30000.	0.171E-01	0.804E-02	0.466E-02	0.335E-02	0.412E-02	0.265E-02
	50000.	0.184E-01	0.671E-02	0.491E-02	0.368E-02	0.430E-02	0.292E-02

Table 1. continued

6s2S-7p2Po3/2	2500.	0.154E-01	0.111E-01	0.449E-02	0.253E-02	*0.403E-02	*0.190E-02
Au I 164.67 nm	5000.	0.172E-01	0.124E-01	0.481E-02	0.306E-02	*0.429E-02	*0.236E-02
C=0.33E+18	10000.	0.187E-01	0.126E-01	0.516E-02	0.360E-02	0.454E-02	0.281E-02
	20000.	0.202E-01	0.113E-01	0.558E-02	0.416E-02	0.483E-02	0.327E-02
	30000.	0.212E-01	0.989E-02	0.586E-02	0.450E-02	0.503E-02	0.355E-02
	50000.	0.222E-01	0.824E-02	0.626E-02	0.494E-02	0.530E-02	0.391E-02
6s2S-8p2Po1/2	2500.	0.403E-01	0.272E-01	*0.114E-01	*0.534E-02		
Au I 150.14 nm	5000.	0.453E-01	0.317E-01	*0.124E-01	*0.700E-02		
C=0.19E+18	10000.	0.501E-01	0.326E-01	*0.134E-01	*0.857E-02	*0.118E-01	*0.658E-02
	20000.	0.558E-01	0.277E-01	*0.144E-01	*0.101E-01	*0.126E-01	*0.789E-02
	30000.	0.600E-01	0.241E-01	*0.150E-01	*0.110E-01	*0.131E-01	*0.865E-02
	50000.	0.642E-01	0.200E-01	0.159E-01	0.122E-01	*0.137E-01	*0.964E-02
6s2S-8p2Po1/2	2500.	0.550E-01	0.369E-01				
Au I 149.45 nm	5000.	0.604E-01	0.414E-01	*0.155E-01	*0.926E-02		
C=0.12E+18	10000.	0.651E-01	0.418E-01	*0.169E-01	*0.116E-01		
	20000.	0.705E-01	0.345E-01	*0.185E-01	*0.138E-01	*0.157E-01	*0.107E-01
	30000.	0.741E-01	0.296E-01	*0.195E-01	*0.151E-01	*0.164E-01	*0.118E-01
	50000.	0.770E-01	0.246E-01	*0.210E-01	*0.168E-01	*0.174E-01	*0.132E-01
PERTURBER DENSITY= 1.E+17cm-3							
6s2S-6p2Po1/2	2500.	0.144E-01	0.590E-02	0.942E-02	0.153E-02	0.926E-02	0.119E-02
Au I 267.67 nm	5000.	0.167E-01	0.681E-02	0.953E-02	0.178E-02	0.946E-02	0.140E-02
C=0.12E+21	10000.	0.175E-01	0.696E-02	0.959E-02	0.204E-02	0.953E-02	0.161E-02
	20000.	0.191E-01	0.625E-02	0.963E-02	0.231E-02	0.957E-02	0.183E-02
	30000.	0.213E-01	0.495E-02	0.966E-02	0.249E-02	0.959E-02	0.197E-02
	50000.	0.259E-01	0.360E-02	0.970E-02	0.272E-02	0.961E-02	0.216E-02
6s2S-6p2Po3/2	2500.	0.164E-01	0.984E-02	0.102E-01	0.248E-02	0.993E-02	0.191E-02
Au I 242.87 nm	5000.	0.192E-01	0.118E-01	0.104E-01	0.292E-02	0.102E-01	0.228E-02
C=0.79E+20	10000.	0.209E-01	0.131E-01	0.105E-01	0.338E-02	0.104E-01	0.266E-02
	20000.	0.230E-01	0.132E-01	0.107E-01	0.386E-02	0.105E-01	0.305E-02
	30000.	0.254E-01	0.134E-01	0.108E-01	0.416E-02	0.105E-01	0.329E-02
	50000.	0.295E-01	0.109E-01	0.109E-01	0.456E-02	0.106E-01	0.362E-02
6s2S-7p2Po1/2	2500.	0.117	0.745E-01				
Au I 166.58 nm	5000.	0.131	0.896E-01	*0.383E-01	*0.178E-01		
C=0.53E+19	10000.	0.145	0.954E-01	*0.416E-01	*0.232E-01		
	20000.	0.160	0.895E-01	*0.446E-01	*0.284E-01	*0.396E-01	*0.218E-01
	30000.	0.171	0.794E-01	*0.465E-01	*0.313E-01	*0.411E-01	*0.243E-01
	50000.	0.184	0.669E-01	*0.491E-01	*0.351E-01	*0.429E-01	*0.275E-01
6s2S-7p2Po3/2	2500.	0.153	0.986E-01				
Au I 164.67 nm	5000.	0.172	0.116				
C=0.33E+19	10000.	0.187	0.120	*0.510E-01	*0.301E-01		
	20000.	0.202	0.109	*0.556E-01	*0.374E-01		
	30000.	0.212	0.973E-01	*0.585E-01	*0.415E-01	*0.500E-01	*0.321E-01
	50000.	0.222	0.821E-01	*0.625E-01	*0.468E-01	*0.529E-01	*0.365E-01
6s2S-8p2Po1/2	2500.	*0.401	*0.219				
Au I 150.14 nm	5000.	0.452	0.279				
C=0.19E+19	10000.	0.501	0.297				
	20000.	0.558	0.259				
	30000.	0.600	0.230				
	50000.	0.642	0.196				
6s2S-8p2Po1/2	2500.	*0.545	*0.279				
Au I 149.45 nm	5000.	*0.602	*0.350				
C=0.12E+19	10000.	0.649	0.369				
	20000.	0.704	0.315				
	30000.	0.740	0.278				
	50000.	0.769	0.239				

Table 1. continued

PERTURBER DENSITY= 1.E+18cm-3						
6s2S-6p2Po1/2	2500.	0.144	0.561E-01	*0.810E-01	*0.124E-01	*0.676E-01	*0.903E-02
Au I 267.67 nm	5000.	0.167	0.661E-01	*0.906E-01	*0.157E-01	*0.852E-01	*0.119E-01
C=0.12E+22	10000.	0.175	0.681E-01	0.942E-01	0.189E-01	*0.920E-01	*0.146E-01
	20000.	0.191	0.614E-01	0.957E-01	0.221E-01	*0.946E-01	*0.173E-01
	30000.	0.213	0.487E-01	0.963E-01	0.240E-01	0.953E-01	0.189E-01
	50000.	0.259	0.356E-01	0.968E-01	0.266E-01	0.958E-01	0.210E-01
6s2S-6p2Po3/2	2500.	0.163	0.913E-01	*0.835E-01	*0.178E-01	*0.657E-01	*0.121E-01
Au I 242.87 nm	5000.	0.192	0.113	*0.974E-01	*0.243E-01	*0.892E-01	*0.179E-01
C=0.79E+21	10000.	0.209	0.128	*0.103	*0.303E-01	*0.990E-01	*0.231E-01
	20000.	0.230	0.130	0.106	0.361E-01	*0.103	*0.280E-01
	30000.	0.254	0.132	0.107	0.395E-01	*0.104	*0.309E-01
	50000.	0.295	0.108	0.109	0.440E-01	0.106	0.346E-01
6s2S-7p2Po1/2	2500.	* 1.14	*0.497				
Au I 166.58 nm	5000.	1.30	0.721				
C=0.53E+20	10000.	1.44	0.830				
	20000.	1.59	0.807				
	30000.	1.70	0.729				
	50000.	1.84	0.616				
6s2S-7p2Po3/2	2500.	* 1.47	*0.581				
Au I 164.67 nm	5000.	* 1.69	*0.872				
C=0.33E+20	10000.	1.85	0.994				
	20000.	2.01	0.949				
	30000.	2.11	0.847				
	50000.	2.21	0.734				
6s2S-8p2Po1/2	2500.						
Au I 150.14 nm	5000.						
C=0.19E+20	10000.	* 4.69	* 2.05				
	20000.	* 5.37	* 1.94				
	30000.	* 5.82	* 1.76				
	50000.	* 6.29	* 1.59				
6s2S-8p2Po1/2	2500.						
Au I 149.45 nm	5000.						
C=0.12E+20	10000.						
	20000.	* 6.45	* 2.12				
	30000.	* 6.92	* 1.93				
	50000.	* 7.32	* 1.80				
PERTURBER DENSITY= 1.E+19cm-3						
6s2S-6p2Po1/2	2500.	1.40	0.468			
Au I 267.67 nm	5000.	1.66	0.595			
C=0.12E+23	10000.	1.75	0.634			
	20000.	1.91	0.581	*0.898	*0.188	
	30000.	2.13	0.459	*0.930	*0.214	
	50000.	2.59	0.336	*0.953	*0.245	
6s2S-6p2Po3/2	2500.	1.59	0.688			
Au I 242.87 nm	5000.	1.90	0.966			
C=0.79E+22	10000.	2.09	1.16			
	20000.	2.30	1.22			
	30000.	2.54	1.25	* 1.03	*0.331	
	50000.	2.95	1.03	* 1.07	*0.390	
6s2S-7p2Po1/2	2500.					
Au I 166.58 nm	5000.					
C=0.53E+21	10000.	* 12.1	* 4.30			
	20000.	* 14.4	* 5.20			
	30000.	* 15.8	* 4.90			
	50000.	* 17.4	* 4.60			

Table 2. This table shows electron-impact broadening parameters for Au II, calculated within the modified semiempirical approach (Dimitrijević & Konjević 1980; Dimitrijević & Kršljanin 1986; Popović & Dimitrijević 1996) for a perturber density of 10^{17} cm^{-3} and temperatures from 5 000 up to 50 000 K. Transitions and averaged wavelengths for the multiplet ($\bar{\lambda}$ in nm) are also given. Stark broadening parameters for other pertuber densities may be obtained by linear scaling, taking into account that for sufficiently higher densities a correction for Debye shielding effect (Griem 1974) should be applied

Transition	T (K)	W (nm)	d (nm)
6s(3/2, 1/2) − 6p(3/2, 1/2) $\overline{\lambda} = 201.58$ nm	5000.	0.410E-02	−0.912E-03
	10000.	0.285E-02	−0.643E-03
	20000.	0.197E-02	−0.452E-03
	30000.	0.159E-02	−0.365E-03
	40000.	0.137E-02	−0.313E-03
	50000.	0.123E-02	−0.276E-03
6s(3/2, 1/2) − 6p(3/2, 3/2) $\overline{\lambda} = 175.89$ nm	5000.	0.330E-02	−0.623E-03
	10000.	0.229E-02	−0.435E-03
	20000.	0.159E-02	−0.300E-03
	30000.	0.128E-02	−0.237E-03
	40000.	0.111E-02	−0.198E-03
	50000.	0.100E-02	−0.169E-03
6s(5/2, 1/2) − 6p(5/2, 1/2) $\overline{\lambda} = 208.04$ nm	5000.	0.404E-02	−0.106E-02
	10000.	0.282E-02	−0.754E-03
	20000.	0.195E-02	−0.536E-03
	30000.	0.157E-02	−0.441E-03
	40000.	0.135E-02	−0.385E-03
	50000.	0.121E-02	−0.346E-03
6s(5/2, 1/2) − 6p(5/2, 3/2) $\overline{\lambda} = 174.53$ nm	5000.	0.308E-02	−0.658E-03
	10000.	0.215E-02	−0.464E-03
	20000.	0.149E-02	−0.326E-03
	30000.	0.120E-02	−0.264E-03
	40000.	0.103E-02	−0.226E-03
	50000.	0.927E-03	−0.199E-03
6p(3/2, 1/2) − 7s(3/2, 1/2) $\overline{\lambda} = 235.45$ nm	5000.	0.191E-01	0.816E-02
	10000.	0.133E-01	0.607E-02
	20000.	0.939E-02	0.478E-02
	30000.	0.792E-02	0.449E-02
	40000.	0.720E-02	0.451E-02
	50000.	0.679E-02	0.452E-02
6p(3/2, 3/2) − 7s(3/2, 1/2) $\overline{\lambda} = 283.87$ nm	5000.	0.282E-01	0.116E-01
	10000.	0.196E-01	0.860E-02
	20000.	0.139E-01	0.677E-02
	30000.	0.117E-01	0.638E-02
	40000.	0.106E-01	0.642E-02
	50000.	0.100E-01	0.642E-02
6p(5/2, 1/2) − 7s(5/2, 1/2) $\overline{\lambda} = 226.38$ nm	5000.	0.147E-01	0.387E-02
	10000.	0.103E-01	0.284E-02
	20000.	0.719E-02	0.218E-02
	30000.	0.594E-02	0.200E-02
	40000.	0.528E-02	0.197E-02
	50000.	0.487E-02	0.194E-02
6p(5/2, 3/2) − 7s(5/2, 1/2) $\overline{\lambda} = 286.18$ nm	5000.	0.241E-01	0.585E-02
	10000.	0.168E-01	0.430E-02
	20000.	0.118E-01	0.330E-02
	30000.	0.974E-02	0.304E-02
	40000.	0.865E-02	0.299E-02
	50000.	0.798E-02	0.295E-02